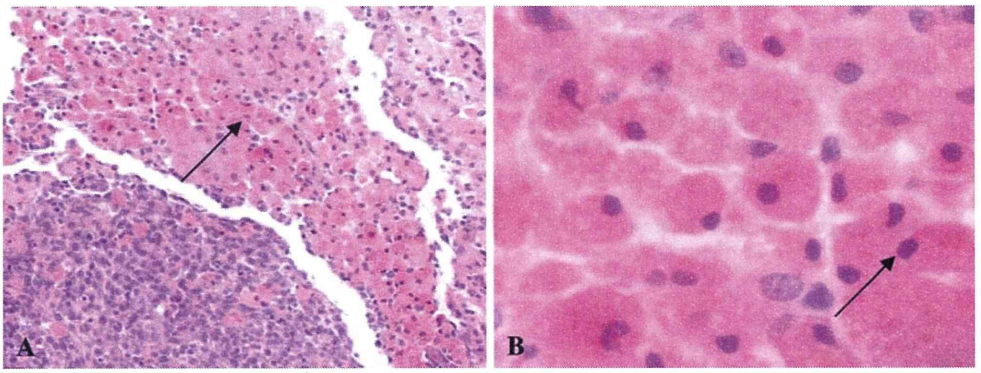

Fig. 5 **A** Low power photomicrograph from the brain of a BNCT treated, F98 glioma bearing rat following administration of H_2TBP by CED. There are large numbers of porphyrin laden macrophages (*arrows*). **B** High power photomicrograph showing porphyrin laden macrophages. These photos were taken at the time of death of the animal at which time they had progressively growing brain tumors

diluting it down to 1% DMSO. Theoretically, bystander killing might occur if the ^{10}B containing macrophages were adjacent to tumor cells. However, the potential lethality of the alpha particles produced as a result of the $^{10}B(n,\alpha)^7Li$ capture reaction would be much less than if they were produced within the tumor cells. Although CED has been effective in improving the distribution of a variety of agents in rats with brain tumors, its effectiveness in humans has been much more problematic [35, 36]. However, as demonstrated in the present study, direct i.c. delivery of therapeutic agents, which bypass the BBB, results in much higher concentrations in the brain tumor and concomitantly lower concentrations in extracranial sites thereby reducing systemic toxicity.

Ozawa et al. [30, 31], as well as we [37], have observed that CED and Alzet pump infusion resulted in significantly higher tumor and lower normal brain boron concentrations than those obtained following systemic administration. They were the first to report that CED significantly increased the tumor uptake of two boronated porphyrins, designated TABP-1 and BOPP, although no BNCT studies were carried out. As shown by us in the present studies, although CED of the carboranylporphyrins has solved the problem of high extracranial tissue uptake by the liver and spleen, the seemingly high tumor boron values did not accurately reflect the true intracellular uptake of the compounds. Direct i.c. administration appears to be the preferred route of administration for the presently available carboranylporphyrins. However, increasing their intracellular localization and homogeneous distribution depend on their physico-chemical properties and mechanism of delivery, which could improve their therapeutic efficacy. Therefore, we currently are synthesizing compounds with enhanced tumor cell uptake. In addition, it would be highly advantageous to have tumor selective compounds that readily cross the BBB, and that could be administered systemically and attain high tumor and low normal brain and extracranial tissue concentrations. It is noteworthy that in vitro studies on the cellular uptake of H_2TCP studies with the murine B16 melanoma [24, 48] cells and H_2TBP with human T98 glioblastoma cells [28] demonstrated intracellular fluorescence of cells that had been incubated with these compounds. Despite their tetra-anionic nature, they were able to penetrate plasma membranes to a certain extent, and may not have formed aggregates, thereby producing intense cellular fluorescence.

Our data provide a cautionary note that high "tumor" boron concentrations do not necessarily mean that the boron delivery agent is localized *within* tumor cells. In the future, we plan to carry out studies using secondary ion mass spectrometry (SIMS) [51] to obtain quantitative data on the boron concentrations of individual tumor cells in tissue sections. This method has been used to determine the cellular and subcellular localization of BPA [52], BSH [53] and carboranyl nucleosides [54]. The challenge will be synthesize and evaluate non-toxic carboranylporphyrins with improved water solubility, which attain high in vivo tumor cell uptake following either systemic injection or direct i.c. administration. Based on the studies of Ozawa et al. [30, 31], Jori, et al. [48] and ourselves, it can be concluded that these compounds are a class of boron delivery agents that warrant further investigation.

Acknowledgments This paper is dedicated to Professor Otto Harling in recognition of his outstanding contributions to the field of BNCT research, and more specifically to his vision and foresight that made the Massachusetts Institute of Technology Research Reactor one of the leading facilities in the world to carry out BNCT studies. Sadly, such studies are no longer being carried out at this facility. We thank Ms. Michelle Van Fossen for expert secretarial assistance in the preparation of this manuscript and Dr. Michael Pennell, Division of Biostatistics, OSU, College of Public Health, for his helpful comments relating to statistical evaluation of the data. The studies described in this report were supported by N.I.H. grants R01 CA098902 (M.G.H.V.) and R01 CA098945 (R.F.B.), and the United States Department of Energy through the program of Innovations in

Nuclear Infrastructure and Education, Office of Nuclear Energy, Science and Technology (contract no. DE-FG07-02ID14420DE-FG07-02, K14420), and the Office of Environmental and Biological Research (contract no. DE-FG02-02ER63358) (K.J.R. and P.J.B.). One of US (RFB) gratefully acknowledges support of The Ohio State University Department of Pathology for partial funding of the final stages of this study.

Conflicts of interest There are no conflicts of interest.

References

1. Vicente MGH (2006) Boron in medicinal chemistry. Anti-cancer Agents Med Chem 6:73
2. Barth RF, Coderre JA, Vicente MGH, Blue TE (2005) Boron neutron capture therapy of cancer: current status and future prospects. Clin Cancer Res 11:3987–4002
3. Sköld K, H-Stenstam B, Diaz AZ et al (2010) Boron neutron capture therapy for glioblastoma multiforme: advantage of prolonged infusion of BPA-f. Acta Neurol Scand 122:58–62
4. Sköld K, Gorlia T, Pellettieri L et al (2010) Boron neutron capture therapy for newly diagnosed glioblatoma multiforme: an assessment of clinical potential. Brit Radio 83:596–603
5. Miyatake S-I, Kawabata S, Yokoyama K et al (2009) Survival benefit of boron neutron capture therapy for recurrent malignant gliomas. J Neurooncol 91:199–206
6. Kawabata S, Miyatake S-I, Kuroiwa T et al (2009) Boron neutron capture therapy for newly diagnosed glioblastoma. J Radiat Res 50:51–60
7. Stupp R, Hegi ME, Mason WP et al (2009) Effects of radiotherapy with concimitant and adjuvant temozolomide versus radiotherapy alone on survival in glioblastoma in a randomised phase UUU study: 5-year analysis of the ORTC-NCIC trial. Lancet Oncol 10:459–466
8. Altieri S, Bortolussi S, Barth RF, Roveda L, Zonta A (2009) Thirteenth international congress on neutron capture therapy. Appl Radiat Isot 67:S1–378
9. Fairchild RG, Kahl SB, Laster BH et al (1990) In vitro determination of uptake, retention, distribution, biological efficacy, and toxicity of boronated compounds for neutron capture therapy: a comparison of porphyrins with sulfhydryl boron hydrides. Cancer Res 50:4860–4865
10. Hill JS, Kahl SB, Kaye AH et al (1992) Selective tumor uptake of a boronated porphyrin in an animal model of cerebral glioma. Proc Natl Acad Sci USA 89:1785–1789
11. Ceberg CP, Brun A, Kahl SB et al (1995) A comparative study on the pharmacokinetics and biodistribution of boronated porphyrin (BOPP) and sulfhydryl boron hydride (BSH) in the RG2 rat glioma model. J Neurosurg 83:86–92
12. Koo MS, Ozawa T, Santos RA et al (2007) Synthesis and comparative toxicology of a series of polyhedral borane anion-substituted tetraphenyl porphyrins. J Med Chem 50:820–827
13. Miura M, Joel DD, Smilowitz HM et al (2001) Biodistribution of copper carboranyltetraphenylporphyrins in rodents bearing an isogeneic or human neoplasm. J Neurooncol 52:111–117
14. Miura M, Micca PL, Fisher CD et al (1998) Evaluation of carborane-containing porphyrins as tumour targeting agents for boron neutron capture therapy. Br J Radiol 71:773–781
15. Miura M, Morris GM, Micca PL et al (2001) Boron neutron capture therapy of a murine mammary carcinoma using a lipophilic carboranyltetraphenylporphyrin. Radiat Res 155:603–610
16. Tibbitts J, Fike JR, Lamborn KR et al (1999) Toxicology of a boronated porphyrin in dogs. Photochem Photobiol 69:587–594
17. Tibbitts J, Sambol NC, Fike JR et al (2000) Plasma pharmacokinetics and tissue biodistribution of boron following administration of a boronated porphyrin in dogs. J Pharm Sci 89:469–477
18. Tsurubuchi T, Yamamoto T, Nakai K et al (2009) Intracellular uptake of a new boronated porphyrin EC032. Appl Radiat Isot 67:94–96
19. Viaggi M, Dagrosa MA, Longhino J et al (2004) Boron neutron capture therapy for undifferentiated thyroid carcinoma: preliminary results with the combined use of BPA and BOPP. Appl Radiat Isot 61:905–909
20. Wu H, Micca PL, Makar MS, Miura M (2006) Total syntheses of three copper (II) tetracarboranylphenylporphyrins containing 40 or 80 boron atoms and their biological properties in EMT-6 tumor-bearing mice. Bioorg Med Chem 14:5083–5092
21. Renner MW, Miura M, Easson MW, Vicente MGH (2006) Recent progress in the syntheses and biological evaluation of boronated porphyrins for boron neutron-capture therapy. Anti-cancer Agents Med Chem 6:145–157
22. Vicente MGH, Sibrian-Vazquez M (2010) Synthesis of boronated porphyrins and their application in BNCT. In: Kadish KM, Smith KM, Guilard R (eds) The handbook of porphyrin science, vol 4, chapter 18. World Scientific Publishers, Singapore, pp 191–248
23. Fabris C, Vicente MGH, Hao E et al (2007) Tumour-localizing and -photosensitising properties of meso-tetra(4-nido-carboranylphenyl)porphyrin (H2TCP). J Photochem Photobiol B 89:131–138
24. Soncin M, Friso E, Jori G et al (2008) Tumor-localizing and radiosensitising properties of meso-tetra(4-nido-carboranylphenyl)porphyrin (H2TCP). J Porphyr Phthalcocya 12:866–873
25. Vicente MGH, Nurco DJ, Shetty SJ et al (2002) Synthesis, dark toxicity and induction of in vitro DNA photodamage by a tetra(4-nido-carboranylphenyl)porphyrin. J Photochem Photobiol B 68:123–132
26. Vicente MGH, Shetty S, Wickramasinghe A, Smith KM (2000) Syntheses of carbon-carbon linked carboranylated porphyrins for application in boron neutron capture therapy. Tetrahedron Lett 41:7626–7627
27. Vicente MGH, Wickramasinghe A, Nurco DJ et al (2003) Synthesis, toxicity and biodistribution of two 5, 15-di[3, 5-(nido-carboranylmethyl)phenyl]porphyrins in EMT-6 tumor bearing mice. Bioorg Med Chem 11:3101–3108
28. Gottumukkala V, Ongayi O, Baker DG et al (2006) Synthesis, cellular uptake and animal toxicity of a tetra(carboranylphenyl)-tetrabenzoporphyrin. Bioorg Med Chem 14:1871–1879
29. Ongayi O, Gottumukkala V, Fronczek FR, Vicente MG (2005) Synthesis and characterization of a carboranyl-tetrabenzoporphyrin. Bioorg Med Chem Lett 15:1665–1668
30. Ozawa T, Afzal J, Lamborn KR et al (2005) Toxicity, biodistribution, and convection-enhanced delivery of the boronated porphyrin BOPP in the 9L intracerebral rat glioma model. Int J Radiat Oncol Biol Phys 63:247–252
31. Ozawa T, Santos RA, Lamborn KR et al (2004) In vivo evaluation of the boronated porphyrin TABP-1 in U-87 MG intracerebral human glioblastoma xenografts. Mol Pharm 1:368–374
32. Yang W, Barth RF, Adams DM et al (2002) Convection-enhanced delivery of boronated epidermal growth factor for molecular targeting of EGF receptor-positive gliomas. Cancer Res 62:6552–6558
33. Morrison PF, Chen MY, Chadwick RS et al (1999) Focal delivery during direct infusion to brain: role of flow rate, catheter diameter, and tissue mechanics. Am J Physiol 277:1218–1229
34. Mardor Y, Rahav O, Zauberman Y et al (2005) Convection-enhanced drug delivery: increased efficacy and magnetic resonance image monitoring. Cancer Res 65:6858–6863
35. Ferguson S, Lesniak MS (2007) Convection enhanced drug delivery of novel therapeutic agents to malignant brain tumors. Curr Drug Deliv 4:169–180

36. Sampson JH, Akabani G, Archer GE et al (2008) Intracerebral infusion of an EGFR-targeted toxin in recurrent malignant brain tumors. Neuro Oncol 10:320–329
37. Kawabata S, Barth RF, Yang W, et al (2006) Evaluation of carboranylporphyrins as boron delivery agents for neutron capture therapy. In: Proceedings for the 12th international congress on neutron capture therapy for cancer. Takamatsu, Japan, pp 123–126
38. Bobadova-Parvanova P, Oku Y, Wickramasinghe A, Hall RW, Vicente MGH (2004) Ab initio and 1H-NMR study of the Zn(II) complexes of a nido- and a close-carboranylporphyrin. J Porphyr Phthalcocya 8:996–1006
39. Newcomb EW, Zugzog D (2009) The murine GL261 glioma experimental mode to assess novel brain tumor treatments, Chap. 12. CNS Cancer. Human press, New York, pp 227–241
40. Barth RF, Adams DM, Soloway AH et al (1991) Determination of boron in tissues and cells using direct-current plasma atomic emission spectroscopy. Anal Chem 63:890–893
41. Ko L, Koestner A, Wechsler W (1980) Morphological characterization of nitrosourea-induced glioma cell lines and clones. Acta Neuropathol 51:23–31
42. Barth RF, Kaur B (2009) Rat brain tumor models in experimental neuro-oncology: the C6, 9L, T9, RG2, F98, BT4C, RT-2 and CNS-1 gliomas. J Neurooncol 94:299–312
43. Barth RF, Yang W, Rotaru JH et al (2000) Boron neutron capture therapy of brain tumors: enhanced survival and cure following blood-brain barrier disruption and intracarotid injection of sodium borocaptate and boronophenylalanine. Int J Radiat Oncol Biol Phys 47:209–218
44. Rogus RD, Harling OK, Yanch JC (1994) Mixed field dosimetry of epithermal neutron beams for boron neutron capture therapy at the MITR-II research reactor. Med Phys 21:1611–1625
45. Barth RF, Wu G, Yang W et al (2004) Neutron capture therapy of epidermal growth factor (+) gliomas using boronated cetuximab (IMC-C225) as a delivery agent. Appl Radiat Isot 61:899–903
46. Madsen RW, Moeschberger ML (1986) Statistical concepts. Prentice-Hall, Englewood Cliffs, NJ
47. Klein JP, Moeschberger ML (2003) Survival analysis techniques for censored and truncated data, 2nd edn. Springer, New York
48. Jori G, Soncin M, Friso E et al (2009) A novel boronated-porphyrin as a radio-sensitizing agent for boron neutron capture therapy of tumours: in vitro and in vivo studies. Appl Radiat Isot 67:321–324
49. Coderre JA, Glass JD, Fairchild RG et al (1987) Selective targeting of boronophenylalanine to melanoma in BALB/c mice for neutron capture therapy. Cancer Res 47:6377–6383
50. Shibata Y, Matsumura A, Yoshida F et al (1998) Cell cycle dependency of porphyrin uptake in a glioma cell line. Cancer Lett 129:77–85
51. Chandra S, Tjarks W, Lorey DR, Barth RF (2008) Quantitative subcellular imaging of boron compounds in individual mitotic and interphase human glioblastoma cells with imaging secondary ion mass spectrometry (SIMS). J Microsc 229:92–103
52. Smith DR, Chandra S, Coderre JA, Barth RF (1997) Quantitative ion microscopy imaging of boron-10 in rat brain tumor models for BNCT. In: Larsson B, Crawford J, Weinrich R et al (eds) Advances in neutron capture therapy, vol II, chemistry and biology. Elsevier Science B.V., Amsterdam, pp 308–314
53. Smith DR, Chandra S, Coderre JA, Morrison GH (1996) Ion microscopy imaging of ^{10}B from p-boronophenylalanine in a brain tumor model for boron neutron capture therapy. Cancer Res 56:4302–4306
54. Barth RF, Yang W, Al-Madhoun AS, Johnsamuel J et al (2004) Boron-containing nucleosides as potential delivery agents for neutron capture therapy of brain tumors. Cancer Res 64:6287–6295

Examination of ^{11}C-Methionine Metabolism by the Standardized Uptake Value in the Normal Brain of Children

Takashi Nagata, Naohiro Tsuyuguchi, Takehiro Uda, Yuzo Terakawa, Toshihiro Takami, and Kenji Ohata

Department of Neurosurgery, Osaka City University Graduate School of Medicine, Osaka, Japan

The aim of this study was to determine the uptake of L-[methyl-^{11}C]-methionine (^{11}C-MET) in the normal brain of patients younger than 20 y, to facilitate more accurate diagnoses in young patients. **Methods:** Eighty-two patients were categorized into 4 groups according to their age. They underwent ^{11}C-MET PET, and a standardized uptake value (SUV) was determined for different brain regions including the frontal lobe, parietal lobe, cerebellum, and brain stem. **Results:** Compared with all other parts of the brain, the cerebellum had the highest SUV. A tendency for a positive relationship between SUV and age was found in all regions, and a significant relationship with SUV was found in the frontal lobe and cerebellum. **Conclusion:** The character of SUV in the normal brains of children is different from that of adults, and these normal SUV data will play an important role as a critical reference value.

Key Words: ^{11}C-methionine PET; normal accumulation; standardized uptake value; children

J Nucl Med 2011; 52:201–205
DOI: 10.2967/jnumed.110.082875

The tracer L-[methyl-^{11}C]-methionine (^{11}C-MET) is useful for PET in neurooncology (*1,2*), making it possible to assess the characteristics of lesions that could not be diagnosed by other means (*1,3–7*). ^{11}C-MET uptake is also informative about the malignancy of lesions, as is ^{18}F-FDG PET (*6,7*). For younger patients, it is critical to get accurate information about lesions, such as the degree of malignancy and extent of lesions, as early as possible. Therefore, it is essential to have an accurate understanding of ^{11}C-MET PET data. To date, ^{11}C-MET PET has been interpreted mainly using the lesion-to-normal (L/N) ratio—comparison between ^{11}C-MET uptake in the lesion and that in the corresponding normal region in the contralateral hemisphere (*8–10*). In cases of a highly malignant lesion, it would be relatively easy to point out where the lesion is, but when the disease has low malignancy, it may be difficult because interpretation of the result is semiquantitative. Thus, an absolute index is desirable. Uda et al. determined the normal ^{11}C-MET uptake and extent of variation (*11*), but there is no report about normal uptake among children. In the current study, we evaluated normal ^{11}C-MET uptake in persons younger than 20 y.

Received Aug. 31, 2010; revision accepted Oct. 21, 2010.
For correspondence or reprints contact: Takashi Nagata, 1-4-3 Asahi-machi, Abeno-ku, Osaka, Japan 545-8585.
E-mail: tnagatam.0222512.ns@gmail.com

MATERIALS AND METHODS

Patients

Between February 1994 and May 2008, 1,228 patients underwent ^{11}C-MET PET at Osaka City University Hospital. Of these patients, 136 were 20 y or younger. Exclusion criteria included the following: infiltrative grade II–IV neoplasm according to the World Health Organization classification (*12*), extramedullary or midline tumors greater than 20 mm in diameter (3 patients), edematous changes in the brain (3 patients), and history of radiation therapy or chemotherapy (48 patients). The remaining 82 patients (40 male and 42 female; mean age ± SD, 12.4 ± 6.1 y; range, 0–20 y), who were not taking any drugs that could influence brain metabolism, were divided into 4 groups according to their age: group 1, 0–5 y; group 2, 6–10 y; group 3, 11–15 y; and group 4, 16–20 y. The standardized uptake value (SUV) of normal brains was examined according to age and each region, including the frontal lobe, parietal lobe, cerebellum, and brain stem.

The Ethics Committee of Osaka City University Graduate School of Medicine approved this PET study. Informed consent was obtained from all patients or their parents.

PET

PET was performed with an Eminence B PET scanner (Shimadzu); the spatial resolution was 4.5 mm (in full width at half maximum), and slice thickness was 5.6 mm. Scans were obtained parallel to the orbitomeatal line of the patients. After 4 h of fasting, ^{11}C-MET (6 MBq/kg) was injected intravenously over 30 s. After a transmission scan was obtained, a static scan of 10 min was begun 20 min after injection.

Imaging Analysis

Two experienced nuclear medicine radiologists interpreted the scans. The PET images were reconstructed by measured attenuation correction. In both analyses, the region of interest (ROI) was placed manually in the axial plane within the frontal cortex, parietal cortex, cerebellum, and brain stem (Fig. 1). The ROIs of these regions, except for the brain stem, were demarcated manually within the lateral side of the gray matter by reference to the MRI data. In the brain stem, the ROI was placed over the whole

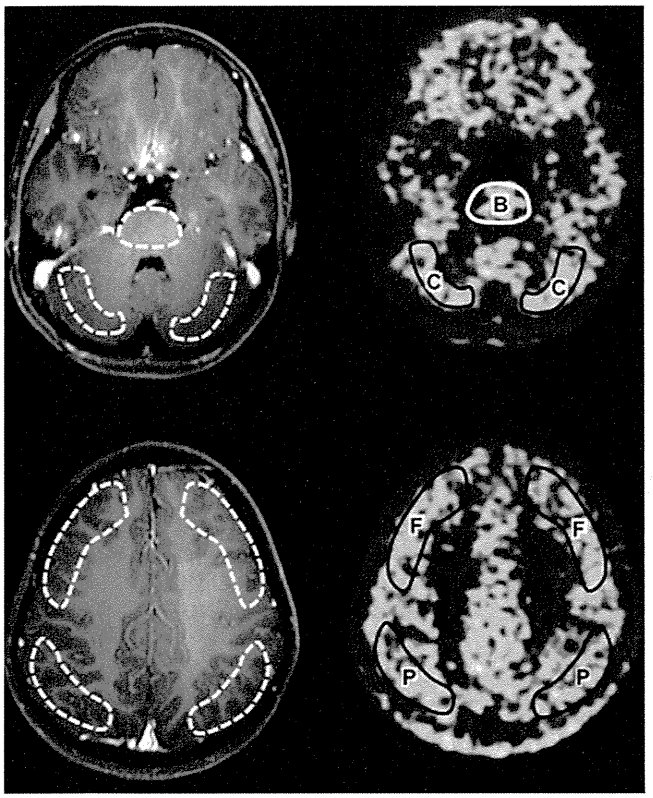

FIGURE 1. Sample of ^{11}C-MET PET images. ROIs were taken manually in axial plane. Coregistration between MR images and PET scans is adequate. B = brain stem; C = cerebellum; F = frontal cortex; P = parietal cortex.

brain stem at the middle pons level. Mean pixel counts in the ROIs were normalized to SUV using the subject's body weight with the following equation: SUV = ([mean pixel count/pixel volume]/[injected radioisotope activity/body weight]) × calibration factor.

Statistical Analysis

The differences between each part of the brain were analyzed in every group. The sample consisted of 54 patients for whom we had all SUV data, including the right frontal lobe, right parietal lobe, right cerebellum, and brain stem. Statistical analysis was performed by non–repeated-measures ANOVA, with post hoc tests corrected using Bonferroni and Student–Newman–Keuls analysis.

The relationship between SUV and age was analyzed in every part of the brain with linear regression and Spearman correlation tests. The samples used in these analyses were 158 frontal hemispheres (79 right hemispheres and 79 left hemispheres), 118 parietal hemispheres (59 right hemispheres and 59 left hemispheres), 156 cerebellar hemispheres (77 right hemispheres and 79 left hemispheres), and 62 brain stems. In all statistical analyses, significance was defined as a P value less than 0.05.

RESULTS

Frontal Lobe

SUVs (mean ± SD) in the frontal lobe were 1.133 ± 0.295 and 1.088 ± 0.379 in group 1, 1.067 ± 0.264 in group 2, 1.101 ± 0.268 in group 3, and 1.199 ± 0.258 in group 4 (Table 1). A significant linear regression between SUV and age ($P = 0.0282$) was found (Fig. 2).

Parietal Lobe

SUVs (mean ± SD) in the frontal lobe were 1.149 ± 0.290 and 1.052 ± 0.399 in group 1, 1.114 ± 0.209 in group 2, 1.122 ± 0.220 in group 3, and 1.235 ± 0.243 in group 4 (Table 1). Significant differences between groups 1 and 4 ($P < 0.01$) were found, but no significant linear regression between SUV and age ($P = 0.396$) was found (Fig. 2).

Cerebellum

SUVs (mean ± SD) in the frontal lobe were 1.312 ± 0.309 and 1.145 ± 0.347 in group 1, 1.319 ± 0.345 in group 2, 1.327 ± 0.301 in group 3, and 1.394 ± 0.251 in group 4 (Table 1). Significant differences between groups 1 and 2 ($P < 0.05$), groups 1 and 3 ($P < 0.01$), and groups 1 and 4 ($P < 0.01$) were found. A significant linear regression between SUV and age ($P = 0.00197$) was also found (Fig. 2).

Brain Stem

SUVs (mean ± SD) in the frontal lobe were 1.245 ± 0.306 and 1.096 ± 0.367 in group 1, 1.222 ± 0.165 in group 2, 1.268 ± 0.3422 in group 3, and 1.298 ± 0.265 in group 4 (Table 1). No statistically significant difference between SUV and age was found (Fig. 2).

Comparison Between Each Part of Brain

Fifty-four of the 82 patients were analyzed, and significant differences between the frontal lobe and cerebellum ($P < 0.01$), frontal lobe and brain stem ($P < 0.01$), parietal lobe and cerebellum ($P < 0.05$), and parietal lobe and brain stem ($P < 0.05$) were found (Fig. 3). In group 3, significant

TABLE 1
SUV in Each Part of Brain in Every Group

	Frontal lobe		Parietal lobe		Cerebellum		Brain stem	
Group	*n*	Mean ± SD	*n*	Mean ± SD	*n*	Mean ± SD	*n*	Mean ± SD
1	36	1.088 ± 0.379	30	1.052 ± 0.399	35	1.145 ± 0.347	11	1.096 ± 0.367
2	14	1.067 ± 0.264	12	1.114 ± 0.209	12	1.319 ± 0.345	6	1.222 ± 0.165
3	46	1.101 ± 0.268	28	1.122 ± 0.220	46	1.327 ± 0.301	20	1.268 ± 0.3422
4	62	1.199 ± 0.258	48	1.235 ± 0.243	63	1.394 ± 0.251	25	1.298 ± 0.265
Total	158 (right, 79; left, 79)	1.133 ± 0.295	118 (right, 59; left, 59)	1.149 ± 0.290	156 (right, 77; left, 79)	1.312 ± 0.309	62	1.245 ± 0.306

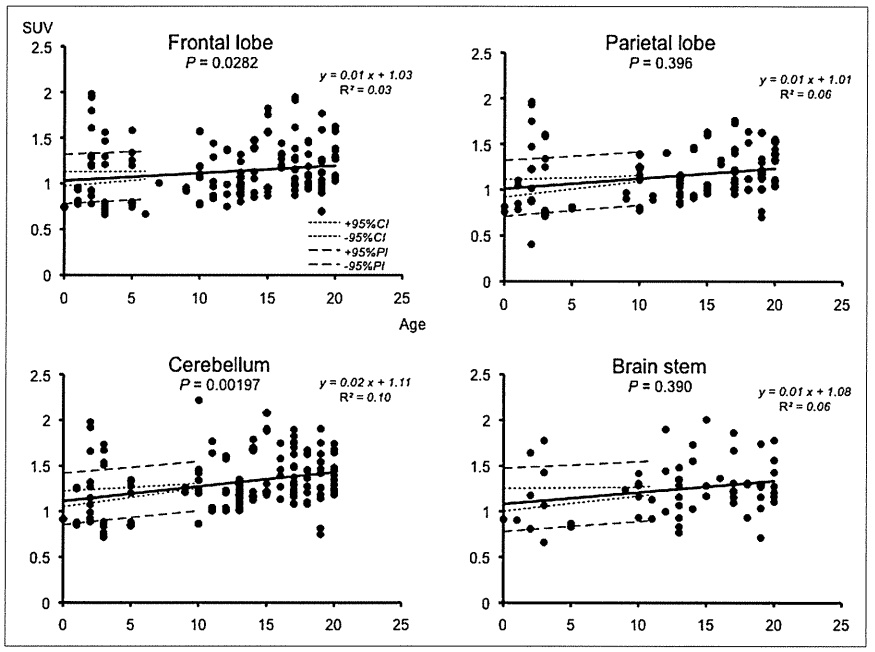

FIGURE 2. Regression and scatterplots for analysis of age-associated SUV change in frontal lobe, parietal lobe, cerebellum, and brain stem. In all parts of brain, positive linear regression was found, but *P* value of regression coefficient was statistically significant only in frontal lobe and cerebellum.

differences between the frontal lobe and cerebellum ($P < 0.01$) and frontal lobe and brain stem ($P < 0.01$) were found. But in groups 1, 2, and 4, there was no significant difference between each part of the brain (Fig. 4).

DISCUSSION

^{11}C-MET PET has been used for the description of lesions and for less invasive evaluation of malignancy. Many papers show that PET is more sensitive and specific than MRI in detecting intracranial tumors (*6,9,10*), because PET can detect amino acid metabolism in various cells directly. In general, amino acid metabolism is low in normal brain tissue and high in tumor tissue. According to this difference in ^{11}C-MET accumulation, ^{11}C-MET PET can display clear contrast images for lesions. Therefore, ^{11}C-MET PET would be an informative modality for detecting the boundary between an active lesion and normal brain tissue (*6*). Some reports have also described ^{18}F-FDG PET as being helpful in assessing the degree of malignancy (*3–6*), and ^{11}C-MET PET is also associated with malignancy and may provide valuable information on clinical tumor aggressiveness and prognosis (*6,7,13*).

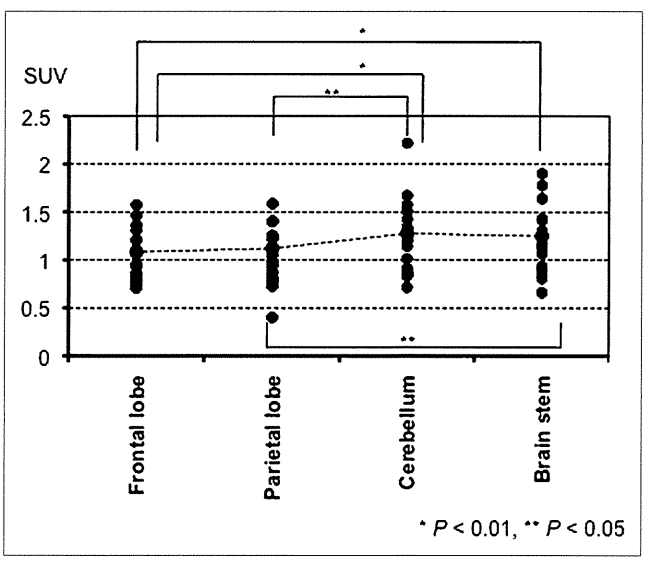

FIGURE 3. SUV in different parts of brain among patients aged 0–20 y. Significant differences between frontal lobe and cerebellum, frontal lobe and brain stem, parietal lobe and cerebellum, and parietal lobe and brain stem were observed.

In general, ^{11}C-MET PET images have been evaluated mainly by using an L/N ratio that compares ^{11}C-MET uptake in the lesion with that in the corresponding normal region in the contralateral hemisphere (*8–10*). Because the reference normal tissue will influence the result of the L/N ratio as a denominator, it is important that an appropriate location be chosen for the ROI used to calculate the normal reference value (*14*).

There are variations in normal ^{11}C-MET accumulation for each part of the brain and variation between different ages (*11*). The reliability of the L/N ratio will, then, decline when uptake in the lesion is not so high. In addition, in the case of tumors near the midline or brain stem, it will be difficult to set normal ROIs in the contralateral region. Therefore, it is important to know the absolute amount of SUVs in the normal brain.

In a previous study, Uda et al. reported the SUV in the normal adult brain (*11*), and such data are an important indicator of amino acid metabolism. To date, there has been no report about normal uptake of ^{11}C-MET in brains throughout development, including infancy, childhood, and

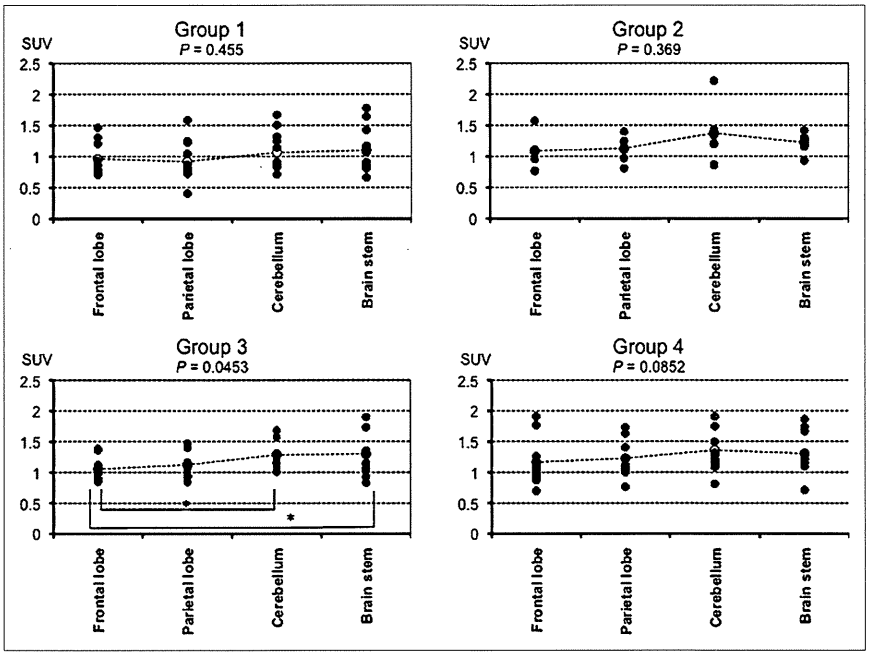

FIGURE 4. SUV in different brain parts in every group. In group 1, SUV was highest in brain stem, followed by cerebellum, but significant difference was not observed. In group 2, SUV was highest in cerebellum but also was not statistically significantly different from other regions. In group 3, significant differences between frontal lobe and cerebellum and frontal lobe and brain stem were found. In group 4, although SUV was highest in cerebellum, difference was not statistically significant. *$P < 0.01$.

young adulthood. If standard amino acid metabolism varies by age, the SUV may be a more suitable indicator than the L/N ratio in ^{11}C-MET PET.

In previous reports, O'Tuama et al. showed a significant age-dependent decline of ^{11}C-MET uptake in maturing adults (*15*), and Uda et al. also reported a slightly negative linear regression, although no statistically significant difference was observed (*11*). The reason for this age-associated decline in ^{11}C-MET uptake was explained as a developmental decline in the activity of the neutral amino acid transporter of the blood–brain barrier (*15*). In the present study, we found that uptake of ^{11}C-MET in all parts of the brain we studied gradually increased with age until 20 y, possibly reflecting high activity of the neutral amino acid transporter and brain protein synthesis to meet the needs of brain metabolism. These results suggest that the brains of younger persons are immature and still developing.

On the other hand, ^{18}F-FDG PET, the local cerebral metabolic rate for glucose, is higher in infants at 3–5 mo old (*16,17*). This tendency is different from our result in ^{11}C-MET PET because the metabolism of glucose represents not only the activity of neurocytes but also the activity of the neural network, including structures around synapses, whereas amino acid metabolism indicates the extent of protein synthesis. ^{11}C-MET uptake also increases linearly as the brain matures during young adulthood. After brain weight reaches a plateau, the uptake begins to decrease, reflecting developmental decline, as described in a previous report (*15*).

In each part of the brain, SUV was highest in the cerebellum in this population, similar to results reported for adult humans investigated by Uda et al. (*11*). The plasticity of synapses is important for motor learning (*18*), which is critically governed by the cerebellum. Activity of the neural network will increase amino acid metabolism in neurocytes, and this higher motor learning will continue for a lifetime. In addition, there is higher cell density in the cerebellum, especially in the granular cell layer, than is found in other brain regions. Therefore, total amino acid metabolism will increase. These are possible reasons for high accumulation in the cerebellum.

We obtained more reliable information about ^{11}C-MET SUV in normal brains, including age-associated and regional changes. This study provides useful information for clinical determinations such as operative indications, which are affected by the malignancy of the lesion.

When continuous long-term follow-up is necessary in some children and younger patients, information about normal metabolism variation associated with aging is useful in making judgments regarding the effectiveness of treatment, and thus it is essential to make accurate evaluations according to a patient's age and brain region.

CONCLUSION

The present study evaluated the accumulation of ^{11}C-MET and SUVs in the normal brain among children and young adults and found significant age-associated differences in some regions. To make more accurate evaluations in ^{11}C-MET PET, age-associated criteria will be necessary in children and young adults.

REFERENCES

1. De Witte O, Goldberg I, Wikler D, et al. Positron emission tomography with injection of methionine as a prognostic factor in glioma. *J Neurosurg.* 2001;95:746–750.
2. Kato T, Shinoda J, Oka N, et al. Analysis of ^{11}C-methionine uptake in low-grade gliomas and correlation with proliferative activity. *AJNR.* 2008;29:1867–1871.

3. Goldman S, Levivier M, Pirotte B, et al. Regional methionine and glucose uptake in high-grade gliomas: a comparative study on PET-guided stereotactic biopsy. *J Nucl Med.* 1997;38:1459–1462.
4. Kaschten B, Stevenaert A, Sadzot B, et al. Preoperative evaluation of 54 gliomas by PET with fluorine-18-fluorodeoxyglucose and/or carbon-II-methionine. *J Nucl Med.* 1998;39:778–785.
5. Levivier M, Massager N, Wikler D, et al. Use of stereotactic PET images in dosimetry planning of radiosurgery for brain tumors: clinical experience and proposed classification. *J Nucl Med.* 2004;45:1146–1154.
6. Pirotte BJ, Lubansu A, Massager N, et al. Clinical interest of integrating positron emission tomography imaging in the workup of 55 children with incidentally diagnosed brain lesions. *J Neurosurg Pediatr.* 2010;5:479–485.
7. Utriainen M, Metsahonkala L, Salmi TT, et al. Metabolic characterization of childhood brain tumors: comparison of F-18-fluorodeoxyglucose and C-11-methionine positron emission tomography. *Cancer.* 2002;95:1376–1386.
8. Terakawa Y, Tsuyuguchi N, Iwai Y, et al. Diagnostic accuracy of ^{11}C-methionine PET for differentiation of recurrent brain tumors from radiation necrosis after radiotherapy. *J Nucl Med.* 2008;49:694–699.
9. Tsuyuguchi N, Sunada I, Iwai Y, et al. Methionine positron emission tomography of recurrent metastatic brain tumor and radiation necrosis after stereotactic radiosurgery: is a differential diagnosis possible? *J Neurosurg.* 2003;98:1056–1064.
10. Tsuyuguchi N, Takami T, Sunada I, et al. Methionine positron emission tomography for differentiation of recurrent brain tumor and radiation necrosis after stereotactic radiosurgery: in malignant glioma. *Ann Nucl Med.* 2004;18:291–296.
11. Uda T, Tsuyuguchi N, Terakawa Y, Takami T, Ohata K. Evaluation of the accumulation of ^{11}C-methionine with standardized uptake value in the normal brain. *J Nucl Med.* 2010;51:219–222.
12. Louis DN, Ohgaki H, Wiestler OD, et al. The 2007 WHO classification of tumours of the central nervous system. *Acta Neuropathol.* 2007;114:97–109.
13. Kato T, Shinoda J, Nakayama N, et al. Metabolic assessment of gliomas using ^{11}C-methionine, [^{18}F] fluorodeoxyglucose, and ^{11}C-choline positron-emission tomography. *AJNR.* 2008;29:1176–1182.
14. Coope DJ, Cizek J, Eggers C, Vollmar S, Heiss WD, Herholz K. Evaluation of primary brain tumors using ^{11}C-methionine PET with reference to a normal methionine uptake map. *J Nucl Med.* 2007;48:1971–1980.
15. O'Tuama LA, Phillips PC, Smith QR, et al. L-methionine uptake by human cerebral cortex: maturation from infancy to old age. *J Nucl Med.* 1991;32:16–22.
16. Suhonen-Polvi H, Ruotsalainen U, Kinnala A, et al. FDG-PET in early infancy: simplified quantification methods to measure cerebral glucose-utilization. *J Nucl Med.* 1995;36:1249–1254.
17. Chugani HT, Phelps ME. Maturational changes in cerebral function in infants determined by ^{18}F-FDG positron emission tomography. *Science.* 1986;231:840–843.
18. Boyden ES, Katoh A, Raymond JL. Cerebellum-dependent learning: the role of multiple plasticity mechanisms. *Annu Rev Neurosci.* 2004;27:581–609.